

PAPER • OPEN ACCESS

Absorption and emission properties of ruby ($\text{Cr:Al}_2\text{O}_3$) single crystal

To cite this article: H H Kusuma *et al* 2019 *J. Phys.: Conf. Ser.* **1170** 012054

View the [article online](#) for updates and enhancements.



IOP | ebooksTM

Bringing you innovative digital publishing with leading voices to create your essential collection of books in STEM research.

Start exploring the collection - download the first chapter of every title for free.

Absorption and emission properties of ruby (Cr:Al₂O₃) single crystal

H H Kusuma^{1,*}, B Astuti² and Z Ibrahim³

¹ Physics Department, Universitas Islam Negeri Walisongo Semarang, Semarang, Indonesia

² Physics Department, Universitas Negeri Semarang, Semarang, Indonesia

³ Physics Department, Universiti Teknologi Malaysia, Johor Bahru, Malaysia

*Corresponding author: hamdanhk@walisongo.ac.id

Abstract. Absorption and emission measurement were made on ruby (Cr:Al₂O₃) crystal with 0.5 wt. %). The results for optical absorption spectra of Cr³⁺:Al₂O₃ single crystal are shows two strong absorption bands at 408 nm and 558 nm in the range spectrum between 390 nm and 600 nm, meanwhile three broad absorption bands at 205 nm, 227 nm and 255 nm in range spectrum between 190 nm and 370 nm. The emission band when excited by UV light at 205 nm, 227 nm and 255 nm were detected and centered at 321 nm. The emission band by the excitation of 408 nm was found at 465 nm, 671 nm, 692 nm and 710 nm. Meanwhile, the emission band under the excitation of blue light at 490 nm was detected at 671 nm, 692 nm and 710 nm. The emission band at 671 nm, 688 nm, 695 nm and 710 nm were detected from excitation by green light with wavelength at 532 nm and 558 nm.

1. Introduction

Sapphire crystal is being an important technological material as lasing material in solid state lasers [1]. The presence of impurities in a crystal can influence its spectroscopic, mechanical, semiconducting, superconducting, magnetic, dielectric and transport properties [2]. Doping sapphire with foreign ions can be used to modify the optical properties and makes the system useful for large variation application, such us tunable solid state laser [3] and optical waveguides [4-6]. Sapphire becomes a promising material for tunable lasers if doped with elements possessing wide absorption bands and wide emission regions [7]. The transition-metal ions are also excellent alternatives and they are widely used in laser crystals [8]. The transition metals, lose the outer 4s electrons and possible some 3d electrons in forming ionic bonds; their resulting electronic configurations are 1s²2s²2p⁶3s²3p⁶3dⁿ where n<10. Ions with incomplete 3d shells have a number of low lying energy levels between which optical transitions may occur. Since the optically active 3d electrons are outside the ion core they interact strongly with electric fields of nearby ions. In order to obtain the energy levels of the 3dⁿ ions at the crystal-field sites, the interaction of the 3d electrons with the neighboring ions must be taken into account [9].

The trivalent chromium (Cr³⁺) ion is an important transition metal member group. Cr³⁺ ion with its 3d³ electron configuration has a very attractive combination of the spin-quartet and spin doublet states. Two different situations can occur for an excited state are depending on the crystal field strength [10-12] (i) the first excited is the spin-quartet ⁴T_{2g}. This corresponds to a weak or medium crystal field,



with broad ${}^4T_{2g} \rightarrow {}^4A_{2g}$ emission band. (ii) the first excited state is the spin-doublet 2E_g . This is the strong crystal field case, with very sharp ${}^2T_g \rightarrow {}^4A_{2g}$ luminescence line. Cr^{3+} ion is widely used as an active ion for solid state lasers. It has received the considerable attention of researches since 1960, when the laser generation was realized with Al_2O_3 . Chromium doped Al_2O_3 commonly referred to as ruby.

Ruby is a very important crystal not only for its applications in optics, but also for its nobleness in gemstones. It can act as a laser medium and make a visible light laser, which possesses many good properties such as narrow line width, long fluorescent lifetime, large quantum efficiency and very wide absorption band. Besides, the host crystal corundum makes its physical–chemical properties excellent [13]. Ruby has the following several advantages as an active medium [7] namely a high pulse power, possibility of operation at room temperature, the highest mechanical strength compared with other laser media, good photochemical resistance to pump source radiation and the high threshold of surface and bulk damage under the influence of its own radiation.

The spectroscopic properties of the transition metal ions in a laser material are characterized mainly by absorption and emission band structures. Some relatively narrow line features may be superimposed on the broad absorption and emission bands. These transitions are referred to as the vibronic transitions because they involve the simultaneous absorption or emission of both photons and phonons. Since the laser host material is strongly involved in the absorption and emission processes, the nature of the transition metal lasers depends strongly on the laser material itself [14]. In the paper, we report on the results of a complex study of $\text{Cr}^{3+}:\text{Al}_2\text{O}_3$ crystals, which includes optical absorption, emission spectroscopy and schematic energy level diagram.

2. Materials and Methods

The polycrystalline trivalent chromium (Cr^{3+}) powder (0.5 wt. %) doped sapphire (Al_2O_3) was used to grow the ruby crystal. The $\text{Cr}^{3+}:\text{Al}_2\text{O}_3$ crystal was grown using the Cz method with ADC system and was prepared and polished for measurement of absorption, and emission spectroscopy. The absorption spectrum measurement was made using a Shimadzu-u 3101PC UV-VIS NIR spectrophotometer. A Perkin Elmer Instruments model LS 55 Luminescence Spectrometer has been used to investigate the excitation and emission spectra of the crystal. The experiments were performed at room temperature.

3. Result and Discussion

The optical absorption spectra of $\text{Cr}^{3+}:\text{Al}_2\text{O}_3$ single crystal is shown in Figure 1. It shows two strong absorption bands at 408 nm and 558 nm in the range spectrum between 390 nm and 600 nm, meanwhile three board absorption bands at 205 nm, 227 nm and 255 nm in range spectrum between 190 nm and 370 nm. The optical absorption of $\text{Cr}^{3+}:\text{Al}_2\text{O}_3$ is similar to the optical absorption of $\text{V}^{3+}:\text{Al}_2\text{O}_3$. These bands are similar to that reported by Song *et al*, [13]. They observed the optical absorption spectrum of $\text{Cr}^{3+}:\text{Al}_2\text{O}_3$ at 206 nm, 225 nm, 255 nm, 410 nm and 550 nm and the crystal was grown by TGT. Yang *et al*, [8] observed two board absorption band centered on 409 nm and 549 nm and strongest absorption band peaked at 209 nm and 222 nm.

From the result, the typical absorption peaks of Cr^{3+} doped in Al_2O_3 (ruby) near 408 nm and 558 nm are corresponding to the energy transition ${}^4A_2 \rightarrow {}^4T_1$ and ${}^4A_2 \rightarrow {}^4T_2$, respectively (Figure 1). The weak absorption peak R_1 and R_2 near 693 nm was also detected. The strong absorption below peak 300 nm in the ultraviolet region, at 205 nm is related F center and two small humps can be seen at the slightly low energy of 227 nm and 255 nm are F^+ centers [13], which is due to the oxygen vacancies during the growth process. This phenomenon is similar to Al_2O_3 single crystal that was described above.

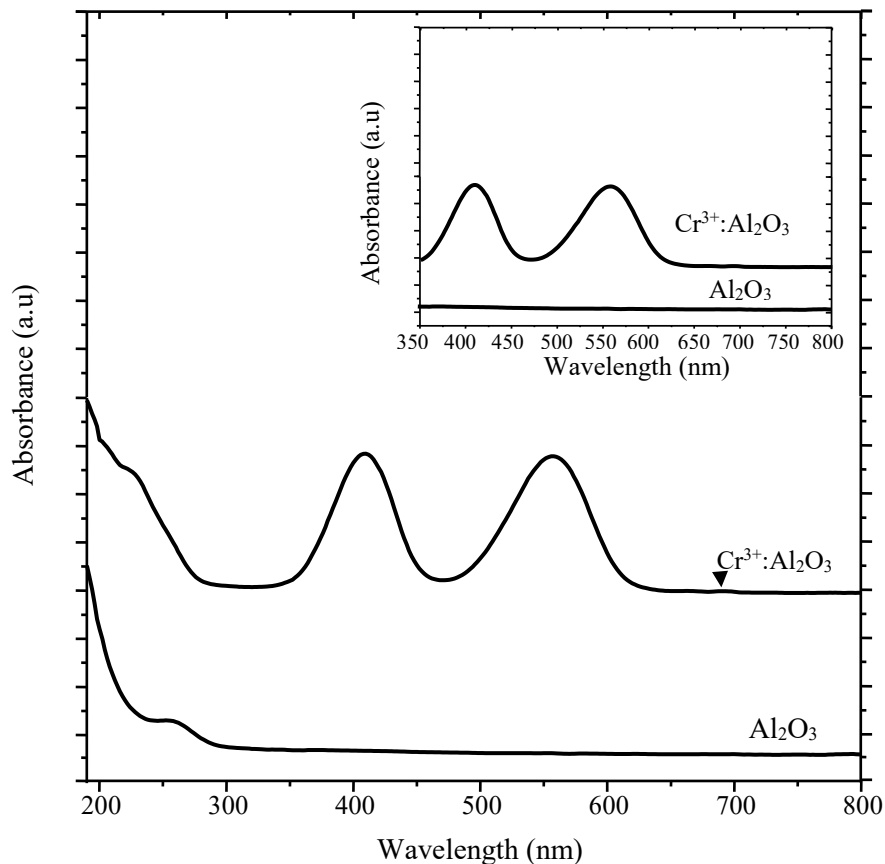


Figure 1. The room temperature optical absorption spectrum of pure Al_2O_3 and Cr^{3+} dopant on Al_2O_3 single crystals.

The luminescence spectrum of $\text{Cr}^{3+}:\text{Al}_2\text{O}_3$ single crystal under different excitation at room temperature ($T=300\text{K}$) is shown in Figure 2 and the position of the peak in Table 1. The fluorescence spectra of $\text{Cr}^{3+}:\text{Al}_2\text{O}_3$ have been detected using an excited UV light with wavelengths around 205 nm, 227 nm and 255 nm, excited using violet light at 408 nm and excited by blue-green light with the wavelength around 490 nm, 532 nm and 558 nm. The emission band when excited by UV light at 205 nm, 227 nm and 255 nm were detected and centered at 321 nm. The emission band by the excitation of 408 nm was found at 465 nm, 671 nm, 692 nm and 710 nm. Meanwhile the emission band under the excitation of blue light at 490 nm was detected at 671 nm, 692 nm and 710 nm. The emission band at 671 nm, 688 nm, 695 nm and 710 nm were detected from excitation by green light with wavelength at 532 nm and 558 nm.

Table 1. The emission band peak position of $\text{Cr}:\text{Al}_2\text{O}_3$ single crystal under different wavelength excitation.

Compounds (Sample Name)	Average Peak Position of Emission Band under Different Wavelength Excitation (nm)			
	205, 227 & 255	408	490	532 & 558
Cr: Al_2O_3	321	-	-	-
	-	465	-	-
	-	671	671	671
	-	692	692	688
	-	-	-	695
		710	710	710

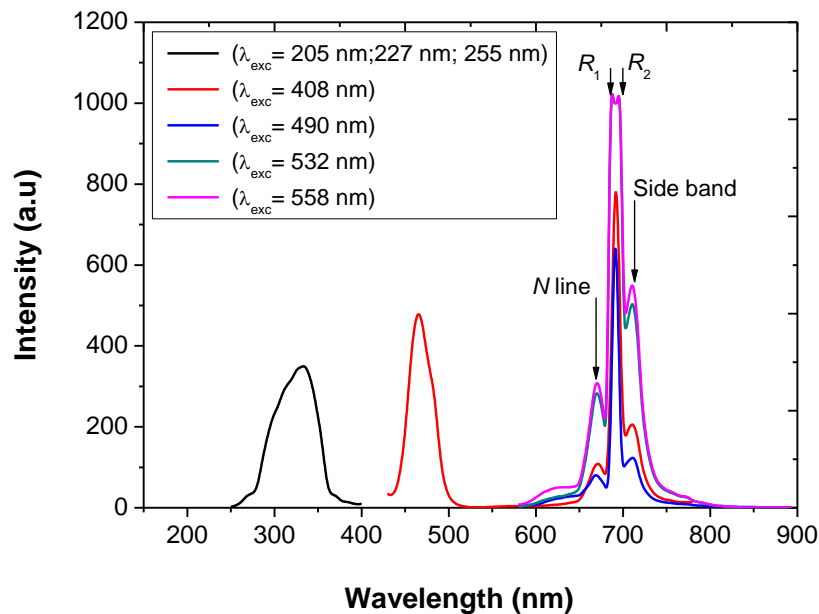


Figure 2. Emission spectrum of $\text{Cr}^{3+}:\text{Al}_2\text{O}_3$ single crystal under different wavelength excitation.

From the result, the emission band near 321 nm might come from oxygen ion vacancies as assigned to the characteristic emission of Cr^{4+} that is stimulated through charge-transfer transition is usually attributed to F^+ centers (anion vacancy with one trapped electron). The emission bands at around 465 nm in the region blue-green of 460 nm – 560 nm might come from F_2 center [15].

The emission spectrum from $\text{Cr}^{3+}:\text{Al}_2\text{O}_3$ under green light (532 nm and 558 nm) has double peaks broad R line at 688 nm and 695 nm which is attributed to R - lines (Raman lines R_1 and R_2) of Cr^{3+} and showed fluorescence at 671 nm in attributed to N - lines (neighbor lines) and the 710 nm is due to the side bands [16]. The emission spectrum of $\text{Cr}^{3+}:\text{Al}_2\text{O}_3$ is dominated by R_1 and R_2 bands and assigned to the well known radiative transition ${}^2E \rightarrow {}^4A_2$ in Cr^{3+} ions in octahedral crystal field. The existence of two R -lines is caused by splitting of the 2E excited state due to spin-orbit coupling [16]. The results are in agreement with earlier reported values [17, 18]. The R_1 and R_2 lines are known to be originated due to $3d^{3n*} \rightarrow 3d^{3n}$ transition of Cr^{3+} [18]. When light is incident on the Cr^{3+} ion, an electron is raised from its ground state 4A_2 to its excited state (4T_2 and 4T_1) lying roughly at 2.2 eV and 3.0 eV above the ground state 4A_2 , respectively. These states decay non-radiatively by phonon emission until it ends its lowest excited 2E meta-stable state which on a transition to 4A_2 ground state release photons of wavelength 694 nm and 688 nm. 2E meta-stable is further split into \bar{E} and $2\bar{A}$ states due to the spin orbit interaction [19]. This meta-stable level split into two sub level with a separation of $\Delta E = 47 \text{ cm}^{-1}$. The upper sublevel is the $2\bar{A}$ and the lower one is the \bar{E} sublevel due to transitions from $2\bar{A} \rightarrow {}^4A_2$ and $\bar{E} \rightarrow {}^4A_2$, respectively.

The upper sublevel $2\bar{A}$ and lower level \bar{E} are referred to as the R_1 and R_2 lines, which are located at the end of the visible region at 688 and 695 nm, respectively. The schematic energy level for R line of Cr^{3+} is shown in Figure 3. The splitting of the 2E excited state is the reason for the wavelength different the R_1 and R_2 (Figure 3b) which is due to the Stoke effect in the $\text{Cr}^{3+}:\text{Al}_2\text{O}_3$. The shift of the R_1 and R_2 line can be attributed to tapering band gap in the crystal field, i.e. in relationship with the octahedral oxygen-coordinated Cr^{3+} , under the influence of a deviatory residual stress [17]. The emission spectra for the $\text{Cr}^{3+}:\text{Al}_2\text{O}_3$ single crystal was measured and interpreted into a band model

system. Figure 3. show the band model under different excitation of $\text{Cr}^{3+}:\text{Al}_2\text{O}_3$ crystal and schematic energy level diagram for R lines of Cr^{3+} ions in Al_2O_3 crystal.

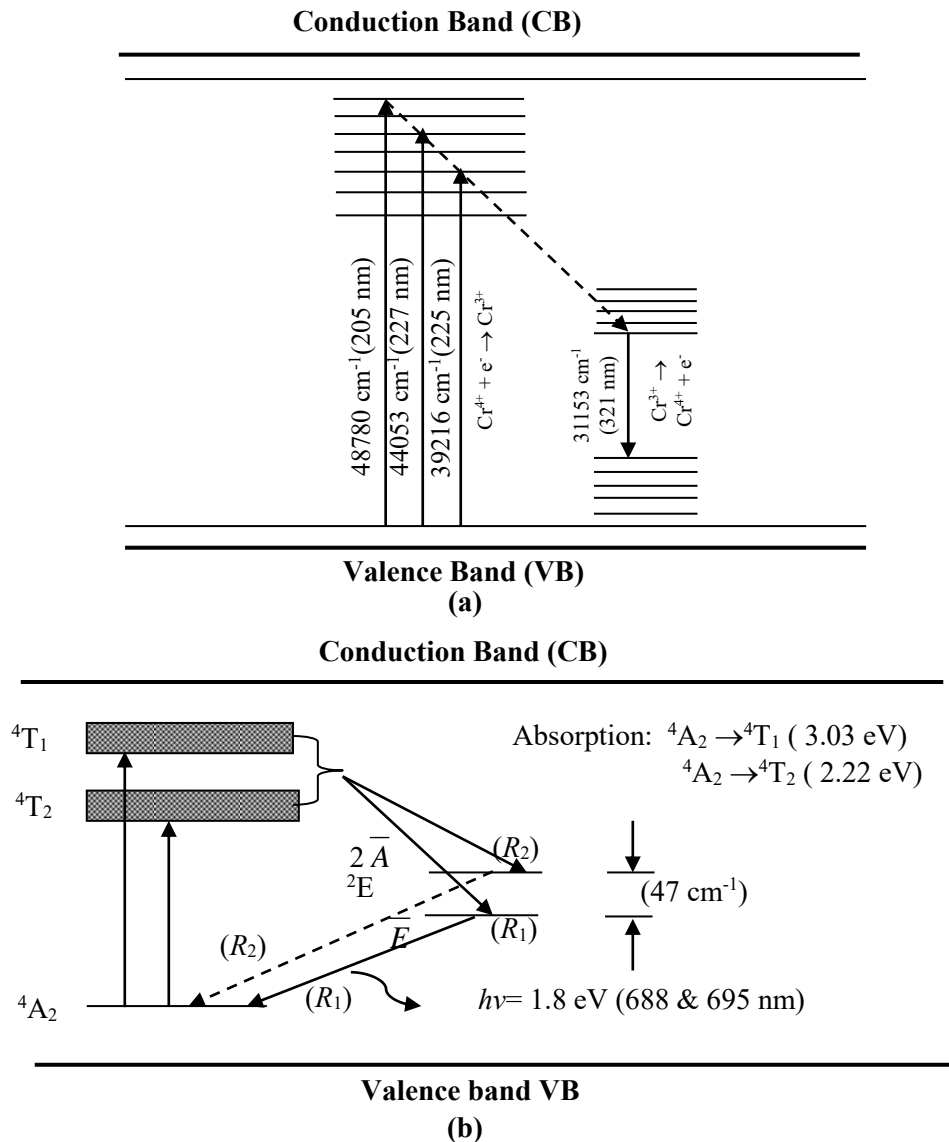


Figure 3. (a) The Band model for $\text{Cr}^{3+}:\text{Al}_2\text{O}_3$ single crystal under different excitation mechanism; (b) The schematic energy level diagram for R lines of Cr^{3+} ions.

4. Conclusion

The optical absorption of $\text{Cr}^{3+}:\text{Al}_2\text{O}_3$ showed two strong absorption bands at 408 nm and 558 nm which corresponded to the energy transition $4A_2 \rightarrow 4T_1$ and $4A_2 \rightarrow 4T_2$, respectively. While the absorption bands at 205 nm which related to the F center and 227 nm and 255 nm are related to the F^+ centers. The emission band of $\text{Cr}^{3+}:\text{Al}_2\text{O}_3$ crystal was found at ~ 321 nm might come from oxygen ion vacancies and assigned to the characteristic emission of Cr^{4+} (attributed to F^+ centers). The emission bands at ~ 465 nm in the region blue-green of 460 nm – 560 nm might come from F_2 center. The emission bands at 688 nm and 695 nm are attributed to R -lines (Raman lines R_1 and R_2) of Cr^{3+} . The

emission spectrum of $\text{Cr}^{3+}:\text{Al}_2\text{O}_3$ is dominated by R_1 and R_2 bands and assigned to the well known radiative transition of ${}^2E \rightarrow {}^4A_2$ in Cr^{3+} ions in the octahedral crystal field.

Acknowledgement

The author wish to thank to the Universiti Teknologi Malaysia for the financial support and Physics Department, UIN Walisongo Semarang for helpful suggestions.

References

- [1] Burton H, Debardelaben C, Amir W and Planchon T A 2017 *Opt Express* **25**(6) 6954
- [2] Gaudry E, Cabaret D, Saintavit P, Brouder C, Mauri F, Goulon J and Rogalev A 2005 *J Phys: Condens Matter* **17** 5467
- [3] Kusuma H H, Ibrahim Z and Saidin M K 2011 *J Appl Sci* **11** 888
- [4] Kusuma H H, Ibrahim Z and Othaman Z 2018 *J Phys: Conf Ser* **983** 012018
- [5] Alombert-Goget G, Sen G, Pezzani C, Barthalay N, Duffar T and Lebbou K 2016 *Opt Mater* **61** 21
- [6] Alombert-Goget A, Lebbou K, Barthalay N, Legal H and Cheriaux G 2014 *Opt Mater* **36** (12)
- [7] Dobrovinskaya E R, Lytvynov L A and Pishchik V 2009 *Sapphire: Material, Manufacturing, Applications* (New York: Springer Science+Business Media)
- [8] Wei Q and Yang Z Y 2009 *J Magn Magn Mater* **321**(12) 1875
- [9] Avram N M and Brik M G 2013 *Optical Properties of 3D Ions in Crystals: Spectroscopy and Crystal Field Analysis* (Beijing: Tsinghua University Press, Beijing) p.215
- [10] Trager F 2012 *Laser and Optics* (New York: Springer-Verlag) p 757
- [11] Henderson B and Bartram R H 2000 *Crystal Field Engineering of Solid State Laser Materials*. (New York: Cambridge University Press)
- [12] Brik M G, Lebedev V A and Stroganova E V 2007 *J Phys Chem Solids* **68** 1796
- [13] Song C, Hang Y, Xia Ch, Xu J and Zhou G 2005 *Opt Mater* **27** 699
- [14] Henderson B and Imbush G F 1989 *Optical Spectroscopy of Inorganic Solids* (Oxford: Clarendon)
- [15] Zhang J, Li-Bin L, Li-Zhang L, Shi-Ji J, Guang-Can W, Yong L and Shou-Yong J 1998 *Nucl Instrum Methods Phys Res B* **141** 446
- [16] Gugushev C, Gotze J and Gobbels M 2010 *Am Mineral* **99** 449
- [17] Pan C, Chen S Y and Shen P 2008 *J Cryst Growth* **310** 699
- [18] Nagabhushana H, Umesh B, Nagabhushana B M, Lakshminarasappa B N, Singh F and Chakradhar R P S 2009 *Spectrochimica Acta Part A: Mol Biomol Spectrosc* **73** 637
- [19] Ma`iman T H, Hoskins R H, D'Haenens I J, Asawa C K and Evthov V 1962 *Phys Rev B* **123** 1151